Jurnal Polimesin
Department of Mechanical Engineering
State Polytechnic of Lhokseumawe
http://e-jurnal.pnl.ac.id/polimesin
e-ISSN : 2549-1999 No. : 5 Month : October
p-ISSN : 1693-5462 Volume : 23 Year : 2025

Processing dates: received on 2025-09-17, reviewed on 2025-10-04, accepted on 2025-10-07 and online availability on 2025-10-31

Hydrometallurgical extraction of TiO_2 from iron sand for industrial raw material

Sony Sukmara[1*], Azwar Manaf[2], Wisnu Ari Adi[3], Adi Ganda Putra[4]

[1]Faculty of Technology and Informatics, Universitas Mathla'ul Anwar Banten. Banten. Indonesia
[2]Department of Physics, Faculty of Mathematics and Natural Sciences, Universitas Indonesia
[3]Centre for Technology of Nuclear Industry Materials, National Nuclear Energy Agency, Indonesia
[4]Faculty of Manufacturing Technology, Jenderal Achmad Yani University
*Corresponding Author: sukmara.sony007@gmail.com

Abstract

Titanium dioxide (TiO_2) is an essential raw material widely used in Indonesia's medical, cosmetic, paint, cement, aerospace, and defense industries. Despite its industrial importance, domestic TiO_2 production remains limited, resulting in continued dependence on imports. Meanwhile, Indonesia possesses abundant iron sand resources that have not been fully utilized as potential raw materials for TiO_2 extraction. This study aims to extract TiO_2 from iron sand obtained from the southern coast of Lebak Regency, Banten Province. The extraction process began with the preparation of iron sand through washing, drying, and magnetic separation to isolate titanium-rich minerals, mainly ilmenite ($FeTiO_3$) and titanomagnetite (Fe_2TiO_4). The ilmenite concentrate was leached using sulfuric acid (H_2SO_4, 96%) at 150–200 °C, forming titanium oxysulfate ($TiOSO_4$) and ferrous sulfate ($FeSO_4$). The solution was filtered, and titanium was precipitated as hydrated titanium dioxide ($TiO_2 \cdot H_2O$) through neutralization. The precipitate was washed, dried, and calcined at 500 °C to obtain anatase-phase TiO_2. X-Ray Diffraction (XRD) analysis revealed dominant mineral phases of ilmenite (98.63%) and titanomagnetite (90.56%), while X-Ray Fluorescence (XRF) showed titanium contents of 22.72% in $FeTiO_3$ and 20.45% in Fe_2TiO_4. The resulting TiO_2 exhibited an anatase phase with 98.7% purity. The findings confirm that Lebak's southern coastal iron sand is rich in titanium-bearing minerals, demonstrating its potential as a sustainable raw material for domestic TiO_2 production. This study provides a preliminary foundation for optimizing the extraction process to enhance yield and support local industrial development.

Keywords:
iron sand, extraction, H_2SO_4 concentration, TiO_2, raw material

1 Introduction

Indonesia is an archipelago with an ocean area of 3257483 km² and a land area of 1922570 km². The archipelago has advantages regarding the potential of its natural resources, which could generate significant foreign exchange reserves, especially iron sand minerals [1][2][3]. Ironically, however, areas with significant natural resources along the coast are still classified as underdeveloped. This is due to a lack of human resources capable of processing and extracting the area's mineral resources. One such area is the coastal region of Lebak Regency, Banten, Indonesia. According to regional geological data, iron sand potential is limited to the southern coastal area of Banten, specifically in Lebak Regency.

Reconstruction of the existing iron sand deposits indicates a distribution area of approximately 12 hectares with a total volume of 64800 tons [4]. Despite its economic potential, iron sand in Lebak Regency has been minimally explored and is mainly used as a construction material. In fact, iron sand contains valuable minerals such as magnetite (Fe_3O_4), hematite (Fe_2O_3), maghemite (γ-Fe_2O_3), ilmenite ($FeTiO_3$), and titanomagnetite ($(FeTi)_2O_4$) [5][6][7], which are potential sources of high-value products such as TiO_2.

Although TiO_2 plays a vital role across various industries, including paint, paper, plastics, aerospace, and healthcare, Indonesia continues to rely heavily on imports to meet its domestic demand. Despite the country's abundant iron sand resources containing titanium-bearing minerals such as ilmenite and titanomagnetite, research and industrial-scale extraction of TiO_2 from these local materials remain limited. The lack of optimized hydrometallurgical processes and insufficient utilization of local raw materials highlight the need for further studies to develop a sustainable route for domestic TiO_2 production. [8][9][10].

Therefore, this study will identify the iron sand content using X-Ray Fluorescence (XRF) technology [11]. XRF is a quantitative and qualitative method with high efficiency for the precise determination of major and trace components in various types of samples. The technique is multi-element, allowing simultaneous determination of multiple elements without chemical separation. In the case of instrumental determination, sample preparation involves only representative methods, such as crushing or homogenization, which minimize contamination risk and speed up the entire analytical process. Furthermore, morphological analysis of the iron sand surface was carried out using a Scanning Electron Microscope (SEM) combined with Energy Dispersive Spectroscopy (EDS) to determine the mineral composition contained in the iron sand [12]. While the determination of the type of minerals contained in the iron sand will be carried out using an X-ray diffractometer, the mineral phase composition will be obtained in weight percentage [13]. The purpose of this study is to identify and analyze the composition of iron sand from Lebak Regency, Banten Province, and to extract TiO_2 on a laboratory scale as an initial step toward developing a pilot-scale and industrial extraction process.

2 Research methodology

This study used iron sand from Binuangen South Beach in Lebak Regency, Banten. First, the iron sand was washed to remove the clay mixture. Then, the clean, dry iron sand was separated mechanically using a magnetic separator. There are two stages of separation using a magnetic separator [14]. In the first stage, a magnetic separator with a weak magnetic field (1000–2000 gauss) is used to obtain iron sand with relatively high iron content. This type of iron sand sample is called X.

The second stage uses a magnetic separator with a strong magnetic field (3000–6000 gauss) to obtain iron sand with a relatively low iron content. This type of iron sand is called Y. Both the X and Y iron sand samples were milled using High-Energy Milling (HEM) for five hours to obtain fine iron sand particles. The samples were then characterized using a Rigaku XRF spectrometer to determine the elemental composition of the iron sand. We observed particle morphology and performed an overall chemical analysis using a SEM and EDS, JED-350, JEOL. The mineral phase analysis of each iron sand sample was carried out qualitatively and quantitatively using a Philips PW1710 X-ray diffractometer with a CuKα X-ray wavelength of 1.5406 Å. Measurements were taken at diffraction angles ranging from 20° to 80° with a step size of 0.02°. The data were analyzed using the General Structure Analysis System (GSAS) program (Rietveld

code). The pseudo-Voigt function was used to refine the diffraction profiles. All characterizations were carried out at the Center for Advanced Materials Science and Technology at the National Nuclear Energy Agency. To make it easier to understand the process of our experiment, we created the research flowchart shown in Fig. 1.

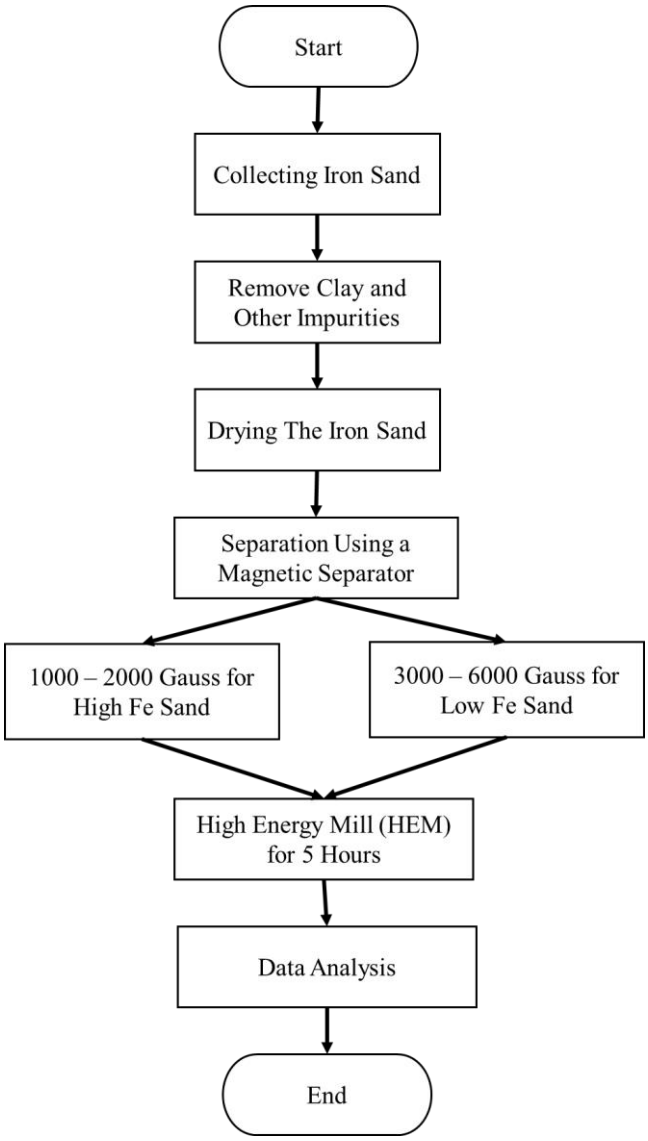

Fig. 1. Experiment flowchart

3 Results and discussion

3.1 Analysis of the elements by using XRF spectrometry

XRF spectroscopy is a technique used to analyze elements in materials or rock minerals based on X-ray interactions. This technique is widely used in rock and mineral analysis because it requires only a few samples to represent a large quantity, provided the material is homogeneous. Additionally, XRF can be used to measure elements primarily found in iron sand or minerals. The sample is typically a powder resulting from milling. In this study, iron sand was milled for five hours to obtain powder with good homogeneity. Table 1 shows the results of the elemental analysis performed using XRF.

Table 1. The result of the elementary analysis of the sample

No.	Element	Content (%)	
		Y	X
1	Fe	65.03	68.00
2	Ti	22.72	20.45
3	Mg	5.28	4.67
4	Al	2.20	3.05
5	Si	2.92	1.87
6	Ca	0.90	0.50
7	S	0.03	0.06
8	P	0.14	0.16
9	Cl	0.03	0.02
10	Cr	0.50	0.04
11	Mn	0.03	0.06
12	Co	0.21	1.02
13	Zn	0.01	0.10

Table 1 shows that samples X and Y contain the following dominant elements: iron (Fe), titanium (Ti), calcium (Ca), sulfur (S), and silicon (Si). Eight minor elements contain less than 1% by weight. Since the dominant element is iron, it is suspected that this iron sand contains magnetite minerals, which may be iron oxides (such as magnetite and hematite) or may bind with other elements to form minerals like ilmenite, titanomagnetite, titanohematite, pyrite, and ferrosilicate minerals. Macroscopic analysis can be performed using petrographic techniques, and a SEM combined with EDS (SEM-EDS) can be used to observe particle morphology.

3.2 Analysis of morphology by SEM-EDS

Energy-dispersive spectroscopy uses the X-ray spectrum emitted by a solid sample bombarded with a focused electron beam to provide localized chemical-element analysis. In principle, all aspects from atomic number Z = 4 (Be) to Z = 92 (U) can be detected, although not all instruments are explicitly equipped for light elements (Z < 10).

Based on the surface morphology and particle shape, it is suspected that there are differences in mineral phases. For this reason, smaller area spots were examined, as shown in Fig. 2. The spot area, as wide as position (003) in Fig. 2(a) obtained results showing that the dominant X-ray spectrum lines are the elements Si and O. In Fig. 2(b), the dominant X-ray spectrum results in the spot area (002), which indicates the elements Ca, C, and O. Thus, the results of this EDS analysis can support further analysis, such as mineral phase analysis using an X-ray diffractometer. Fig. 3 shows a microstructure photograph of (a) TiO_2 Ilmenite and (b) TiO_2 Titanomagnetite. Fig. 3(a) shows that the particles extracted from Ilmenite have a more uniform shape, i.e., they are round. The particle size ranges from 100 – 300 nm; the particles in Ilmenite have agglomerations that tend to be smooth with a reasonably tight distance density. This means that the particles forming TiO_2 undergo a homogeneous process, and the resulting crystals tend to be anatase.

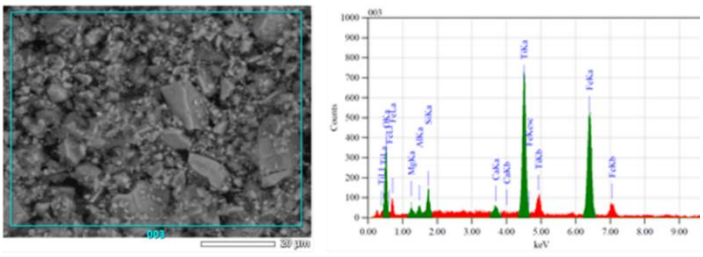

(a) Analysis EDS di spot area (003)

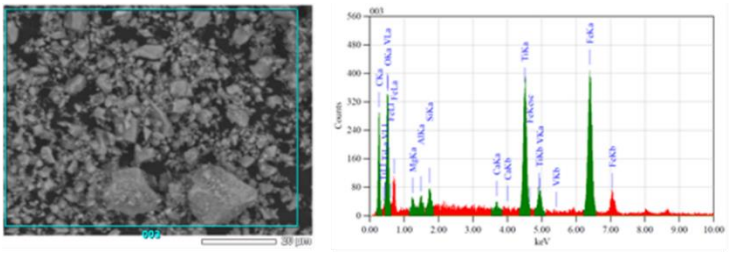

(b) Analysis EDS di sport area (002)

Fig. 2. The result of SEM – SEM-EDS analysis of the sand iron sample

Fig. 3(b) shows that the particles extracted from titanomagnetite are larger, with a size range of 200–500 nm. The particle surface appears denser, so the TiO_2 particles of titanomagnetite show a coarser and heterogeneous morphology compared to the TiO_2 of ilmenite.

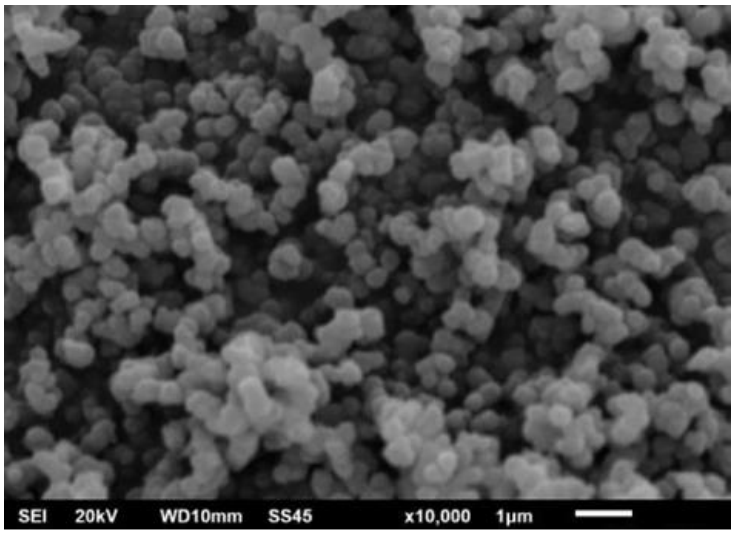

(a)

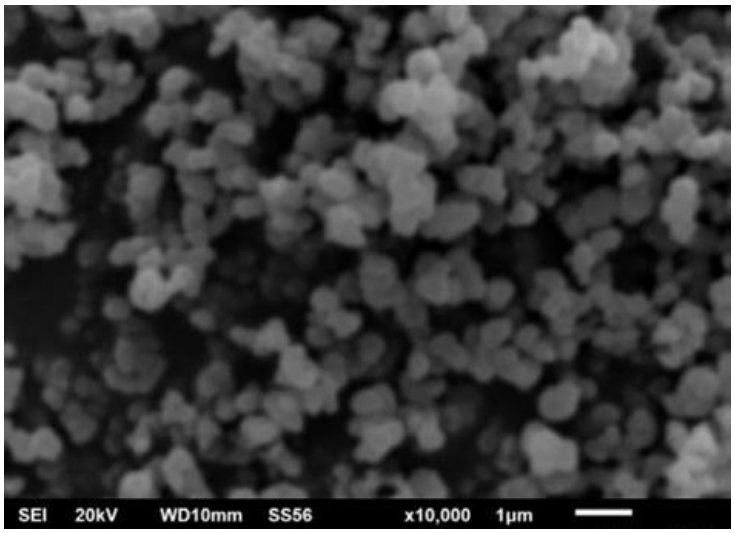

(b)

Fig. 3. Microstructure photograph of (a) TiO_2 ilmenite and (b) TiO_2 titanomagnetite

Table 2 presents the energy-dispersive X-ray spectroscopy (EDS) results for the iron sand samples. Sample Y contains less iron than sample X but exhibits a higher titanium content (28.85% compared to 11.92%). These results indicate that sample Y is richer in the ilmenite phase ($FeTiO_3$), whereas sample X is dominated by titanomagnetite (Fe_2TiO_4), which has a higher iron content.

Table 2. EDS analysis results of iron sand samples

Elements	Energy (keV)	Mass fraction (%)	
		Y	X
Carbon (C)	0.277	-	12.49
Oxygen (O)	0.525	29.46	30.12
Magnesium (Mg)	1.253	1.06	1.83
Alumunium (Al)	1.486	0.31	0.82
Silicon (Si)	1.739	2.61	1.56
Calcium (Ca)	3.690	0.43	1.84
Titanium (Ti)	4.508	28.85	11.92
Vanadium (V)	4.949	-	0.10
Iron (Fe)	6.398	37.28	39.32

3.3 Analysis of the mineral phases by X-Ray Diffraction (XRD)

Fig. 2 shows the XRD measurement results for sample Y. Qualitative analysis revealed that sample Y consists of the ilmenite ($FeTiO_3$) and quartz (SiO_2) mineral phases.

This mineral phase identification is based on the American Mineralogist Crystal Structure Database (AMCSD) [15], which lists the mineral phases ilmenite [16] and quartz [17]. Based on crystallographic data, a quantitative analysis was performed using the GSAS program to determine the structural parameters and the fraction of each mineral phase, as shown in Fig. 4. Fig. 5 shows the refined XRD profile of sample Y, in which ilmenite is the dominant mineral phase. The refinement produced a very good fit with a very small R-factor. The R factor is a criterion for fit, and the goodness-of-fit chi-squared value is also very small. According to Toby, a maximum value of 1.3 is allowed [18]. Several structural parameters of each mineral phase were obtained from the refinement results and are shown in Table 3.

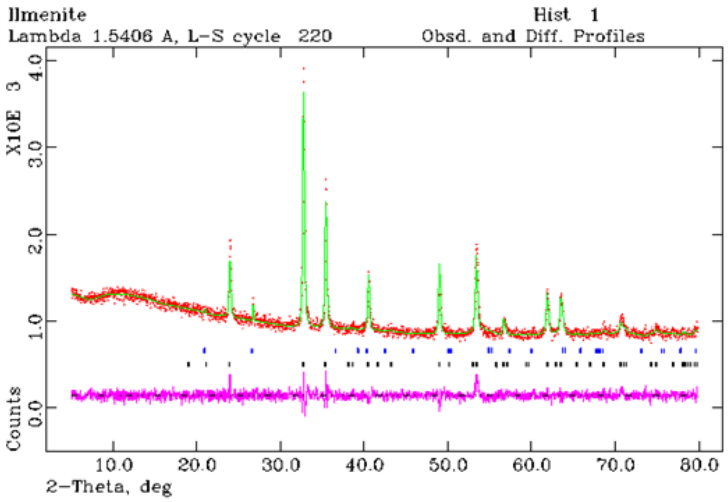

Fig. 4. Identification result of the XRD pattern on the ilmenite sand

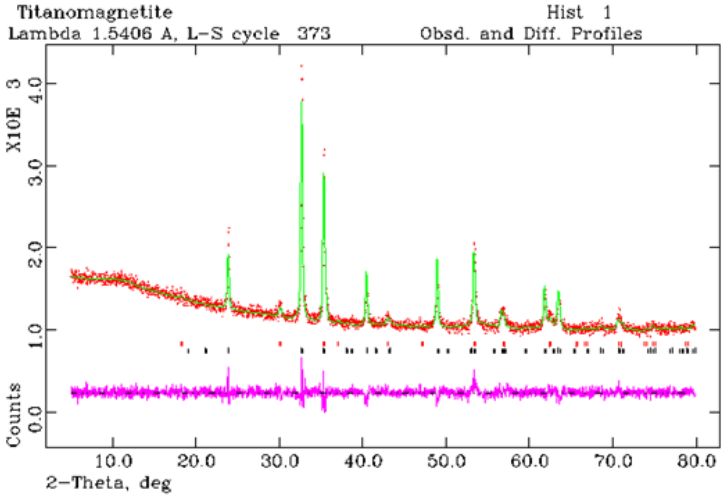

Fig. 5. Identification results of XRD pattern on titanomagnetite sand

Table 3. Structure parameters, mass fraction, and fit criteria of sample Y

Sampel		Y	
Phase (chemical formula)		Ilmenit ($FeTiO_3$)	Quartz (SiO_2)
Mass fraction		98.63 ± 0.001	1.37 ± 0.01
Temperature, T (K)		300 K	300 K
Crystal system		Hexagonal	Hexagonal
Space group		R -3 (148)	P 31 2 1 (152)
Unit cell dimension	a (Å)	5.0721(3)	4.918(2)
	b (Å)	5.0721(3)	4.918(2)
	c (Å)	13.985(1)	5.446(1)
Unit-cell volume, V ($Å^3$)		311.60(6)	114.1(1)
Atomic density, ($gr.cm^{-3}$)		4.941	3.903
Radiation wavelength, λ		1.5406	
Crystal form		Powder	Powder
Color		Gray	White
Goodness-of-fit, χ^2		1.478	
R_{wp} (%)		3.80	

The number of mass fractions of each mineral phase identified from sample Y can be determined according to the crystallographic rules summarized in Table 4. The refinement results yielded several structural parameters for each mineral phase, as shown in Table 5.

Table 4. The mass fraction of phase contents in the sample of ilmenite stone

No.	Mineral name	Phase	Mass fraction (%)

1	Ilmenite	$FeTiO_3$	98.63 ± 0.001
2	Quartz	SiO_2	1.37 ± 0.01

Table 5. Parameter structure, mass fraction, and fit criteria for sample X

Sample		X	
Phase (chemical formula)		Titanomagnetite (Fe_2TiO_4)	Magnetite (Fe_3O_4)
Mass fraction		90.56 ± 0.006	9.44 ± 0.05
Temperature, T (K)		300 K	300 K
Crystal system		Hexagonal	Cubic
Space group		R -3 (148)	F d -3 m (227)
Unit cell dimension	a (Å)	5.0697(4)	8.412(6)
	b (Å)	5.0697(4)	8.412(6)
	c (Å)	13.973(1)	8.412(6)
Unit-cell volume, V ($Å^3$)		311.02(6)	595.4(1)
Atomic density, ($gr.cm^{-3}$)		4.950	4.977
Radiation wavelength, λ		1.5406	
Crystal form		Powder	Powder
Color		Gray	Black
Goodness-of-fit, χ^2		1.483	
R_{wp} (%)		3.46	

As indicated in Table 6, the amount of each mass fraction in the mineral phase of sample X can be determined according to crystallographic rules.

Table 6. The mass fraction of phase contents in the sample of Titanomagnetite stone

No.	Mineral name	Phase	Mass fraction (%)
1	Titanomagnetite	Fe_2TiO_4	90.56 ± 0.006
2	Magnetite	Fe_3O_4	9.44 ± 0.05

Based on the refinement of the XRD patterns of the iron sands named samples X and Y, as well as the supporting data from elementary analysis, petrography, and particle morphology, it is evident that sample Y contains an ilmenite ($FeTiO_3$) mineral phase of 98.03% and a quartz (SiO_2) mineral phase of 1%. 37%. Meanwhile, sample X contains a titanomagnetite ($FeTiO_3$) mineral phase at 90.56% and a magnetite (Fe_3O_4) mineral phase at 9.44%. Therefore, it is expected to serve as a reference for further extraction processes at both the laboratory and industrial scales, thereby increasing local revenue, especially in Lebak Regency.

3.4 Preparation of TiO_2 powder using a hydrometallurgical method.

Table 4 and Table 6 show that the characterized samples are dominated by ilmenite and titanomagnetite. Both ilmenite and titanomagnetite mineral samples contain titanium, so these two samples are considered $FeTiO_3$ Minerals. Then, the $FeTiO_3$ powder was dissolved in 96% concentrated H_2SO_4 [19]. The ilmenite sample to H_2SO_4 ratio was 1:3, with a heating temperature of 110°C and a heating time of 3 hours, in accordance with the equations for Reactions 1 to 3.

$$FeTiO_{3(s)} + 2H_2SO_{4(aq)} \rightarrow FeSO_{4(s)} + TiOSO_{4(aq)} + 2H_2O_{(l)} \quad \text{Reaction 1}$$

$$TiOSO_{4(aq)} + 2H_2O_{(l)} \rightarrow TiO_2.H_2O_{(s)} + H_2SO_{4(aq)} \quad \text{Reaction 1}$$

$$TiO_2.H_2O(s) \rightarrow TiO_{2(s)} + H_2O_{(g)} \quad \text{Reaction 1}$$

In the reduction process, $TiOSO_4$ is separated, and then water is added while stirring with a magnetic stirrer. The mixture is heated to 90°C. In the hydrolysis process, $TiOSO_4$ is added to four liters of water and heated to 100°C. The solution is then cooled until a white $TiO_2 \cdot H_2O$ powder precipitate forms. The precipitate is heated at 500°C to obtain anatase-phase TiO_2. The results of the extraction process were measured using an XRD instrument. Fig. 4 shows the XRD refinement results for the extracted TiO_2 sample, with phase identification according to the Crystallography Open Database (COD) entry 5000223 [20]. Fig. 6 shows that the phase identification of sample X consists of the mineral phases titanomagnetite (Fe_2TiO_4) and magnetite (Fe_3O_4), as determined by XRD measurements.

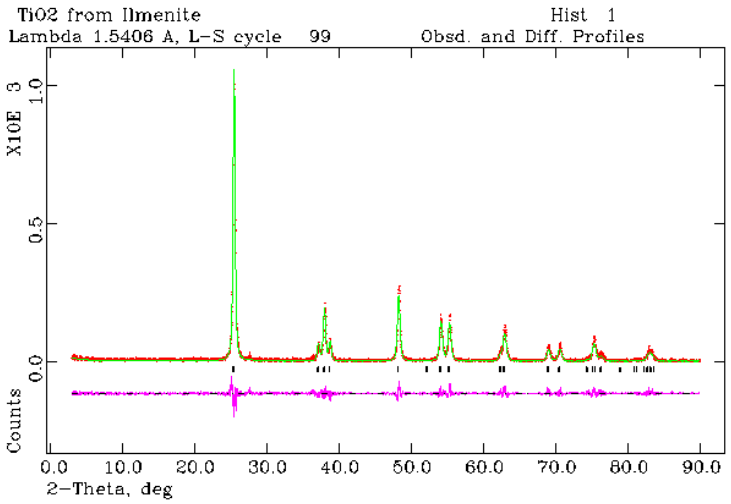

Fig. 6. Smoothing of the XRD profile of the sample X TiO extraction results

Table 7 shows the structural parameters of the XRD pattern refinement results for the TiO_2 sample resulting from the hydrometallurgical process.

Table 7. Structure parameter, factor R, and goodness of fit (χ^2) of the TiO_2 sample

Anatase phase		
Space group: I 41/a m d (141), Crystal system: Tetragonal Lattice parameter: $a = b = 3.7821(2)$ Å, $c = 9.5086(7)$ Å, $\alpha = \beta = \gamma = 90^o$, $V = 136.01(2)$ $Å^3$ and $\rho = 3.902$ $gr.cm^{-3}$		
Factor R	*w*Rp = 2.55	χ^2 (chi-squared) = 1.212
	Rp = 1.68	

Fig. 7 shows the results of refining the XRD pattern of the extracted TiO_2 sample, with phase identification according to the COD 5000223 [20].

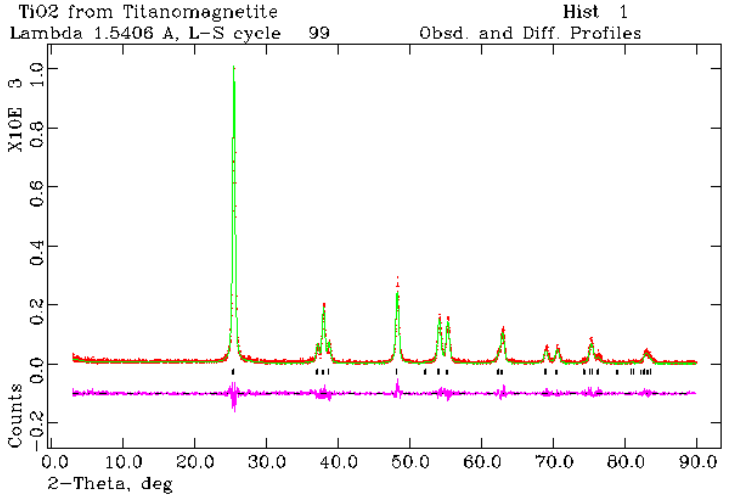

Fig. 7. Smoothing of the XRD profile of the sample Y TiO extraction results

Table 8 shows the structural parameters of the XRD pattern refinement results for the TiO_2 sample resulting from the hydrometallurgical process. Table 7 and Table 8 show that samples of ilmenite and titanomagnetite extracted by the hydrometallurgical method produced anatase-phase TiO_2 raw materials, the purities of which are shown in Table 9. This was determined by elementary testing using XRF spectrometry.

Table 8. Structure parameter, factor R, and goodness of fit (χ2) of the TiO2 sample

Anatase phase
Space group: I 41/a m d (141), Crystal system: Tetragonal Lattice parameter:

$a = b = 3.7825(2)$ Å, $c = 9.5108(7)$ Å, $\alpha = \beta = \gamma = 90^o$, $V = 136.07(2)$ Å^3 and $\rho = 3.900$ gr.cm^{-3}		
Factor R	$wRp = 2.48$	χ^2 (chi-squared) = 1.301
	$Rp = 1.58$	

3.5 Analysis of the elements by using XRF Spectrometry

XRF spectroscopy is a technique used to analyse the elements present in a material or mineral by measuring X-ray interactions. In this study, industrial raw materials were produced by extracting TiO_2 from ilmenite and titanomagnetite. Table 9 presents the results of the XRF elemental analysis.

Table 9. The result of the elementary analysis of the sample

No.	Element	Content (%)	
		Ilmenite	Titanomagnetite
1	Fe	0.07	0.07
2	Ti	98.7	98.7
3	Mg	ND	0.08
4	Al	0.07	0.06
5	Si	0.2	0.25
6	Ca	0.11	ND
7	S	0.11	0.01
8	P	0.01	0.02
9	Sr	0.11	0.1
10	Y	0.01	0.1
11	Pt	0.01	0.01

Based on Table 9, the ilmenite and titanomagnetite samples appear to contain the dominant element, titanium (Ti), at 98.70%. There are also impurity elements present, with a relative content of less than 1%.

Based on the results of XRD and XRF, the results indicate that there is a strong correlation between the mineral phase and the elemental composition, the XRD results show that the ilmenite sample is dominated by the $FeTiO_3$ phase which has a purity of 98.63% and has a quartz phase of 1.37%, while the titanomagnetite sample has a purity of Fe_2TiO_4 90.56% and Fe_3O_4 Phase 9.44%, while the XRF results showed that both particles had the duplicate titanium content of 98.7%, reflecting that the separation and purification process in this experiment was effective, this content is higher when compared to the study from Rahmawati [20], and Firdaus [21] where they took samples on the coast of Lampung, each has a maximum Ti composition of only around 60%. In addition, a study from Suratman [2] and Ishlah [22], who conducted research in Cilacap and Kebumen; their study showed that Ti content in the sand was highest in Kebumen (9.5–25%) and Cilacap (2.28%). This means that TiO_2 produced from lebak with 98.7% purity met industry standards for pigment and catalyst applications, although further purification may be required for advanced optical or photocatalytic applications, where very few impurities can alter the material's optical and electronic properties.

4 Conclusion

The compositional and mineralogical analyses confirm that iron sand from the southern region of Lebak Regency is rich in titanium-bearing minerals, mainly ilmenite ($FeTiO_3$) and titanomagnetite (Fe_2TiO_4). XRD results show that the ilmenite sample is dominated by the $FeTiO_3$ phase (98.63%) with a minor quartz phase (1.37%), while the titanomagnetite sample contains 90.56% Fe_2TiO_4 and 9.44% Fe_3O_4. XRF analysis indicated that both samples have the duplicate titanium content of 98.7%, demonstrating a strong correlation between mineral phases and elemental composition and reflecting the effectiveness of the separation and purification process. The extraction and refinement successfully produced anatase-phase TiO_2 with 98.7% purity, meeting industry standards for pigment and catalyst applications, although further purification may be needed for advanced optical or photocatalytic uses. These results highlight the scientific and industrial significance of Lebak Regency's iron sand as a local source of high-purity TiO_2 and contribute to the development of local titanium resources. Future research should focus on process optimization, maximizing TiO_2 recovery, and evaluating the feasibility of large-scale production to enhance the economic and industrial value of the region's titanium minerals. Additionally, efforts will include scaling up the extraction process, improving efficiency, and further assessing industrial applicability.

ACKNOWLEDGEMENT

We would like to thank Prof. Dr. Azwar Manaf, MSi, and Prof. Dr. Wisnu Ari Adi, MT, for their support in ensuring this research activity ran smoothly.

References

[1] T. Rusianto, M. W. Wildan, K. Abraha, and K. Kusmono, "The potential of iron sand from the coast south of Bantul Yogyakarta as raw ceramic magnet materials," *J Teknol*, vol. 5, no. 1, pp. 62–69, 2012.

[2] H. KURNIO, "Coastal characteristics of iron sand deposits in Indonesia," *Indonesian Mining Journal*, vol. 10, no. 3, pp. 27–38, 2007.

[3] S. Suratman, "distribution characteristics of ferro-titanium oxide mineral on low-grade iron sand," *Indonesian Mining Journal*, vol. 20, no. 1, pp. 49–58, 2017.

[4] A. Manaf, "Kegiatan litbang pasir besi (iron sand) di universitas Indonesia," in *Seminar Lokakarya Pemanfaatan Bahan Baku Lokal untuk Industri baja Nasional, PT Krakatau Steel, Cilegon*, 2005.

[5] T. F. Pramusanto, M. D. Koesnadi, M. A. Satrio, and A. Subandi, "Potensi pemanfaatan bijih besi lokal untuk kemandirian industri baja nasional," in *Proseding Seminar Sehari Bidang Logam MMI 2000*, 2000.

[6] R. Subagja, "Pengalaman pusat penelitian metalurgi LIPI dalam penelitian pemanfaatan bijih besi titan," in *Seminar Lokakarya Pemanfaatan Bahan Baku Lokal untuk Industri Baja Nasional*, 2005.

[7] W. A. Adi and T. R. Mulyaningsih, "Composition analysis of titanomagnetite and ilmenite from iron sand using neutron activation analysis as preliminary study for producing iron oxide and titanium oxide," *Int J Acad Res*, vol. 7, no. 3, pp. 359–364, 2015.

[8] C. Sutowo and F. Rokhmanto, "Sintesis paduan titanium berbasis Ti-Mo-Nb untuk aplikasi biomaterial," *Jurnal Teknik Mesin Cakram*, vol. 6, no. 1, pp. 57–61, Jul. 2023, doi: 10.32493/jtc.v6i1.31807.

[9] R. Muharni and A. S. Dewi, "Corrosion behavior of titanium Ti6Al4V ELI bioceramic coated alloy in artificial saliva modified liquid at fluctuating temperatures," *REM (Rekayasa Energi Manufaktur) Jurnal*, vol. 6, no. 2, pp. 23–27, 2021.

[10] S. S. Priharyono, "Pengambilan titanium dioksida (TiO2) dari pasir besi Kulon Progo dengan metode hidrometalurgi (Variabel Waktu dan Perbandingan Massa)," 2022.

[11] N. Taufiqu Rochman and A. A. Wisnu, "Analysis of structural and microstructure of lanthanum ferrite by modifying iron sand for microwave absorber material application," *Adv Mat Res*, vol. 896, pp. 423–427, 2014.

[12] Y. Aristanti, Y. I. Supriyatna, N. P. Masduki, and S. Soepriyanto, "Decomposition of banten ilmenite by caustic fusion process for TiO2 photocatalytic applications," in *IOP Conference Series: Materials Science and Engineering*, IOP Publishing, 2018, p. 012005.

[13] Y. E. Gunanto, M. P. Izaak, L. Cahyadi, E. Jobiliong, and W. A. Adi, "Preliminary study: Local iron sand characterization of titanomagnetite type," in *IOP Conference Series: Materials Science and Engineering*, IOP Publishing, 2018, p. 012059.

[14] D. Sufiandi, "Konsentrasi pasir besi titan dari pengotornya dengan cara magnetik," *Metalurgi*, vol. 26, no. 1, pp. 15–20, 2015.

[15] D. L. Graf, “Crystallographic tables for the rhombohedral carbonates,” *American mineralogist: Journal of earth and planetary materials*, vol. 46, no. 11–12, pp. 1283–1316, 1961.

[16] Hobart M. King, “Ilmenite,” https://geology.com/minerals/ilmenite.shtml. Accessed on 10 September 2025

[17] Hobart M. King, “Quartz,” https://geology.com/minerals/quartz.shtml. Accessed on 12 September 2025

[18] B. H. Toby, “EXPGUI, a graphical user interface for GSAS,” *Applied Crystallography*, vol. 34, no. 2, pp. 210–213, 2001.

[19] S. Sukmara, W. A. Adi, and A. Manaf, “Mineral analysis and its extraction process of ilmenite rocks in titanium-rich cumulates from Pandeglang Banten Indonesia,” *Journal of Materials Research and Technology*, vol. 17, pp. 3384–3393, 2022.

[20] L. Rahmawati, D. S. Pratama, Z. Sembiring, S. Suharso, T. Anggraeni, and S. Sarwan, “Extraction of titanium dioxide (tio2) from iron sand of tembakak beach west coast as nanoparticles using hydrometallurgy method,” *Analit: Analytical and Environmental Chemistry*, pp. 95–107, 2024.

[21] I. Firdaus, R. Marjunus, and P. Manurung, “Synthesis and characterization of TiO2 from Lampung’s Iron Sand using leaching method with temperature variation,” *Jurnal Fisika dan Aplikasinya*, vol. 17, no. 2, pp. 37–40, 2021.

[22] T. Ishlah, M. R. Parningotan, R. S. Nugraha, T. Handayani, and H. Zahra, “Mineralogy and provenance of titanium-vanadium bearing iron sand deposits from Purworejo-Kebumen, and Cilacap, Central Java.,” *Journal of Mathematical & Fundamental Sciences*, vol. 56, no. 1, 2024.